THE JOURNAL OF PHYSICAL CHEMISTRY B
A JOURNAL OF THE AMERICAN CHEMICAL SOCIETY

pubs.acs.org/JPCB

Article

Local Crowd, Local Probe: Strengths and Drawbacks of Azidohomoalanine as a Site-Specific Crowding Probe

Joseph C. Shirley and Carlos R. Baiz*

Cite This: J. Phys. Chem. B 2024, 128, 5310−5319

Read Online

ACCESS | Metrics & More | Article Recommendations | Supporting Information

ABSTRACT: Every residue on a protein can be characterized by its interaction with water, in lack or in excess, as water is the matrix of biological systems. Infrared spectroscopy and the implementation of local azidohomoalanine (AHA) probes allow us to move beyond an ensemble or surface-driven conceptualization of water behavior and toward a granular, site-specific picture. In this paper, we examined the role of crowding in modulating both global and local behavior on the β-hairpin, TrpZip2 using a combination of Fourier-transform infrared spectroscopy (FTIR) spectroscopy, two-dimensional infrared (2D IR) spectroscopy, and molecular dynamics simulations. We found that, at the amino acid level, crowding drove dehydration of both sheet and turn peptide sites as well as free AHA. However, the subpicosecond dynamics showed highly individualized responses based on the local environment. Interestingly, while steady-state FTIR measurements revealed similar responses at the amino-acid level to hard versus soft crowding (dehydration), we found that PEG and glucose had opposite stabilizing and destabilizing effects on the protein secondary structure, emphasizing an important distinction in understanding the impact of crowding on protein structure as well as the role of crowding across length scales.

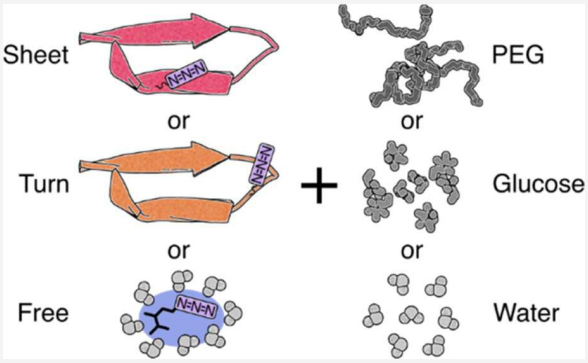

I. INTRODUCTION

Crowding is a biological phenomenon in which the structure and conformational dynamics of a biomolecule are perturbed by the pronounced density of biomolecules. Indeed, biomolecules occupy up to 40% of the cell volume.[1,2] Nonspecific intermolecular interactions and crowding are differences responsible for a schism between conditions *in vitro* versus those *in vivo*; if crowded conditions are removed from an experiment, the observed biomolecular behavior may no longer be representative of the biomolecule *in vivo*.[1,3] Therefore, gaining a fundamental understanding of crowding is essential to enhancing the biological relevance of theoretical and *in vitro* studies.

Crowding interactions have often been divided into "hard" components, which include excluded volume and other steric effects, and "soft" components, which include electrostatics and hydration behavior. These soft interactions, while traditionally overlooked, are not insignificant and have been shown to sometimes have an even greater effect on proteins than steric effects.[4] They have been implicated in destabilizing proteins, altering ligand binding states, and mediating protein−protein interactions.[4,5] While hard interactions are repulsive almost exclusively result of favoring smaller configurations, soft interactions can be either repulsive or attractive depending on the specific interplay between molecules. Of particular importance to soft interactions is the behavior of water in crowded environments because of the direct role water plays in solvation, hydrophobicity, and electrostatics. While the idea of "biological water" is a hot topic that continues to be refined, it is well accepted that proximal water plays a key role in stabilizing biomolecules and mediating their interactions. There is also a notable distinction in the properties of water that is "near" to or "far" from a biomolecule, such as the dielectric constant and water motions.[6,7] In fact, a number of studies have highlighted the impact of interfacial properties, such as local residue polarity, on the structure and dynamics of water. Indeed, water's hydrogen bond network has variable sensitivity to the hydrophobic or hydrophilic nature of that surface.[8] There is a great deal of nuance to be had in the specific and localized interactions between water and biochemical motifs, moving beyond the more generalized effects of surface proximity or quality. This local interplay is quite apparent when the degrees of freedom are minimized, such as within a protein cavity. But even in an expanded capacity, site-specific water-biomolecule interactions remain an important component of the energy landscape. This granular

Received: February 1, 2024
Revised: April 23, 2024
Accepted: May 22, 2024
Published: May 28, 2024

https://doi.org/10.1021/acs.jpcb.4c00712
J. Phys. Chem. B 2024, 128, 5310−5319

interpretation of water becomes increasingly relevant to consider as the importance of local structural dynamics, including those of water, on protein folding, active sites, and protein−ligand interactions has taken center stage.[9−11] Given that crowding alters the structure of water H-bond networks,[12] and with studies demonstrating both the impact of interfaces on water structure and the impact of water structure on proteins, the question arises, what is the interplay between the local protein environment and the crowding effect on water hydrogen bond structural dynamics?

To address this question, it is necessary to probe the local environment of a protein on the same time scale of water dynamics. Two-dimensional infrared (2D IR) spectroscopy is well suited for these measurements for three reasons. First, the time scale, hundreds of femtoseconds to picoseconds, is on the same order as local rearrangements in the water network.[13] Second, the probes, as small as two or three atoms, are minimally perturbative and sensitive to changes in local environment.[14−16] Third, the sensitivity, which scales with the fourth power of the transition dipole moment, is sufficient to measure the system at low concentrations where aggregation is less problematic.[17−20]

Despite the fact that 2D IR spectroscopy is well-suited in time scale and signal strength, crowded environments can confound the interpretation of measurements because within a biological system there are a large number of molecules with highly overlapped peaks, making it difficult to isolate specific components.[21,22] This is because the vibrational modes intrinsic to biomolecules, such as those of amides and carbonyls, are ubiquitous. Furthermore, these modes are often delocalized, restricting their efficacy in interrogating the local environment. One effective solution to these problems has been the implementation of local vibrational probes—minimally perturbative chemical motifs appearing in otherwise unoccupied spectral regions—including nitriles, azides, and thiocyanates.[14,23−26] These probes have been demonstrated as effective tools in various biologically relevant spectroscopic studies including the measurement of protein folding, ligand binding, side-chain solvation, local electrostatics, and metabolism.[14,16,17,24,27] Among nitriles, azidohomoalanine (AHA) is a particularly appealing spectroscopic probe due to its relatively large oscillator strength.[15,16] In addition to being minimally perturbative, vibrational probes provide localized information, and can be installed at various locations in a protein, providing a view of the nearby chemical environment.

In this paper, a site-specific view of the aqueous environment under crowded and uncrowded conditions will be measured. The model system used in this study is the β hairpin peptide TrpZip2. This system was chosen due to its high stability and propensity to remain folded in crowded solutions since the folded state is highly stable.[19,20,28−31] In addition, there has been a wealth of information from computational studies, as the peptide has been used as a model system for simulations.[30] Therefore, the present study aims to establish a relationship between crowding and the local protein environment by installing an azide probe at selected locations within the TrpZip2 peptide and interrogating its behavior under crowded conditions. 2D IR spectroscopy will be used to understand the subpicosecond dynamics of the system. A scheme of the systems studied in this manuscript is shown in Figure 1.

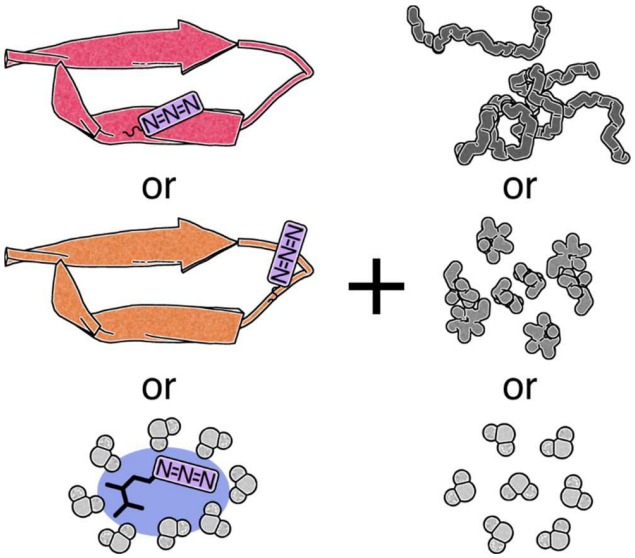

Figure 1. Scheme of the experimental setup for the present work. TrpZip2 labeled at site 10 (red) or site 6 (orange) with AHA (purple) or free AHA (blue) are combined with either PEG solution (dark gray), glucose solution (medium gray), or water (pale gray).

II. METHODS

II.I. Peptides and Sample Preparation. Two TrpZip2 peptide mutants were purchased from WuXi AppTec and treated with HCl to remove trifluoroacetic acid. The studied peptides were Asn6AHA, (SWTWEA*GKWTWK-NH_2), and Thr10AHA (SWTWENGKWA*WK-NH_2), where A* represents azidohomoalanine. Peptide samples were prepared at 5−10 mM concentration in H_2O for Fourier-transform infrared spectroscopy (FTIR) measurements in the azide region and D_2O for measurements in the amide I region to avoid spectral overlap with the solvent. For crowded peptide solutions, 50 μL aliquots of peptide in H_2O/D_2O were first lyophilized to remove solvent, and subsequently reconstituted in crowder solutions. Crowder solutions were prepared gravimetrically by dissolving 400 mg of crowder (glucose or PEG600) in 1 g of H_2O or D_2O at room temperature.

II.II. FTIR Spectroscopy. Samples were placed between two CaF2 windows separated by a 25 μm spacer. Spectra were recorded with 0.5 cm^{-1} resolution at room temperature in H_2O solutions for observation of the azide region. For temperature series data of the amide I region, spectra were taken from 25 to 75 °C in D_2O solutions. FTIR spectra were recorded using a Bruker INVENIO spectrometer. A combination of solution backgrounds and polynomial background subtraction was used to isolate the peaks of interest.[32] Gaussian fits were used to extract the center frequencies and widths of the azide absorption (Table 1).

II.III. Circular Dichroism. Circular dichroism (CD) was used to validate secondary structures of TrpZip2. Samples were diluted to 50 μM peptide concentration from the D_2O-based FTIR samples while maintaining crowder concentration of 400 mg/mL. CD spectra were measured from 190 to 260 nm at 0.5 nm resolution on a Jasco J-815 CD spectrometer in a quartz cuvette with a 1 mm path length. Stock solutions of D_2O + crowder were used for background subtraction.

II.IV. Two-Dimensional Infrared Spectroscopy. To measure local dynamics, two-dimensional infrared (2D IR) spectra in the azide region were measured using a previously

https://doi.org/10.1021/acs.jpcb.4c00712
J. Phys. Chem. B 2024, 128, 5310−5319

Table 1. Center Frequency Shifts with Respect to Free AHA and Peak Widths Reported as the Full Width at Half Maximum (FWHM) are Shown for Free AHA and the TrpZip2 Mutants[a]

	center frequency shift (cm^{-1})	fwhm (cm^{-1})
AHA	0	35.1
AHA + glucose	−0.5	35.5
AHA + PEG	−2.5	36.4
Asn6	−4.8	35.2
Asn6 + glucose	−5.3	36.1
Asn6 + PEG	−6.6	35.6
Thr10	−7.2	34.3
Thr10 + glucose	−7.4	34.2
Thr10 + PEG	−7.8	33.6

[a]These are extracted by single gaussian fits of the azide FTIR. The center frequency of free AHA in H_2O was measured to be 2119 cm^{-1}.

described setup.[33] In brief, a pair of pump pulses was used to excite the sample into a vibrational population. The delay between pump pulses, was scanned from 0 to 3000 fs in steps of 15 fs using a pulse shaper (QuickShape, PhaseTech) using an 1800 cm^{-1} rotating frame. Next, the system and bath were allowed to propagate for a variable waiting time, which was sampled from 250 to 2550 fs (Section SI III) and probed by a third pulse. The signal was dispersed by a grating onto a 128 × 128 pixel MCT array. The sample cells for 2D IR were identical to those used in FTIR, with H_2O as the solvent. The spectra were collected with an edge-pixel referencing scheme to improve the signal-to-noise ratios.[34] Spectra were collected in a magic angle geometry to remove orientational contributions to the measurements. Dynamics were calculated using the nodal line slope (NLS) method.[35] The spectra were interpolated, and nodal points were determined by using sigmoid fitting on pump slices of the spectra. A bootstrapping scheme was used to generate error estimated for the exponential NLS fits.

II.V. Classical Molecular Dynamics Simulations. To aid in the interpretation of 2D IR spectra, classical molecular dynamics simulations were performed with the GROMACS 2021.3 package.[36,37] The CHARMM36m force field was used for all molecules. Topologies were generated by CHARMM-GUI.[38−42] Starting structures for TrpZip2 were obtained from the protein databank and were mutated to contain azidohomoalanine with PyMOL. Boxes were prepared to have 28.6 wt % of crowder in water, not including the mass of the single peptide. The boxes were packed with Packmol and subsequently run through a steepest-descent energy minimization.[43] The boxes were then equilibrated in an NVT ensemble with a velocity-rescaling thermostat for 5 ns. Next, they were equilibrated in the NPT ensemble with a velocity-rescaling thermostat and a cell-rescaling barostat for 100 ns. The systems were then subjected to three sequential production runs with a velocity-rescaling thermostat and Parrinello−Rahman barostat. The first run was 10 ns with frames saved every 1 ps and used for preliminary structural information. The second was for 1 ns with frames saved every 10 fs and used for extracting dynamics. The third was for 200 ns and used to obtain ensemble structural information. Subsequently, 20 100 ps short trajectories were extracted every 10 ns from the 200 ns long trajectory. These short trajectories were used to obtain ensemble ultrafast dynamics. The step size for all equilibration and production stages was 1 fs. Free azidohomoalanine simulations were also prepared in the same way, but without the 200 ns step because the additional statistics were not necessary.

III. RESULTS AND DISCUSSION

III.I. Structure and Stability of TrpZip2. Amide I spectra were measured to confirm properly folded samples for both azide labels under dilute as well as crowded conditions (Figure 2). The measured lineshapes are consistent with antiparallel β-

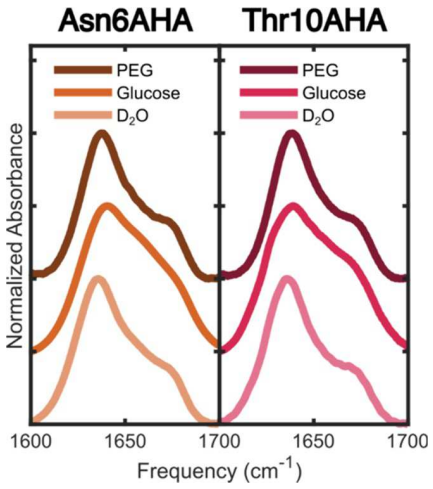

Figure 2. Amide I FTIR of the TrpZip2 mutants in crowded and uncrowded conditions in D_2O. Frequency is on the x-axis and absorbance normalized by maximum is on the y-axis. The spectra are offset by 0.5. The lineshapes for the D_2O and PEG samples match previously reported FTIR of wild-type TrpZip2.[18] The lineshapes in glucose have small deviations, indicative of different hydrogen bonding structures.

sheet formation, with peaks around 1636 and 1672 cm^{-1}. The glucose spectra differ slightly, showing increased intensity in the central region of the amide I band and a slight blue shift in the $\nu_\perp$ band compared to the other samples. The shift is associated with a reduction in the number of coupled residues in the antiparallel β-sheet, whereas the change in the relative population in the central region is due to altered hydrogen bonding within the β-sheet structure. These structural changes in the amide I region of peptides have previously been interpreted as denaturing of the β sheet,[30,44] however, 2D IR studies have shown that TrpZip2, via heating, can undergo H-bonding changes with associated changes in amide I lineshapes, while retaining a large degree of native interstrand contacts.[20] Temperature dependent FTIR, reports on the relative thermal stability of each of the labeled species (Figure 3), confirming that the peptides in glucose are indeed folded at room temperature as discussed next.

There are several trends to interpret from the temperature dependent FTIR spectra (Figures 2 and 3). First, the lineshapes of the D_2O and PEG solutions approach those of the glucose solution as temperature increases. This supports the idea that the room temperature peptide structure is perturbed by glucose in a similar way as would result from heating. There are also similar heating trends between the lineshapes of both mutants as well as between those of water and PEG-crowded samples, namely blueshifting of the band center and changes in population. As with the room temperature FTIR, both changes are in line with a modified

https://doi.org/10.1021/acs.jpcb.4c00712
J. Phys. Chem. B 2024, 128, 5310−5319

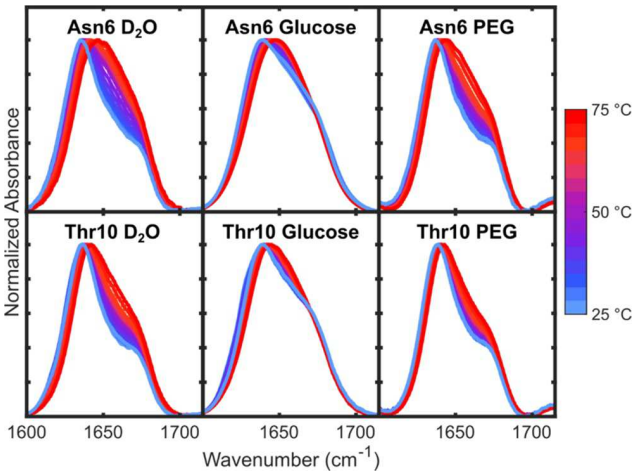

Figure 3. A temperature dependent FTIR of the amide I band for each of the mutants in each crowding solution. Spectra are normalized by maximum. Spectra are colored from low temperature (blue) to high temperature (red).

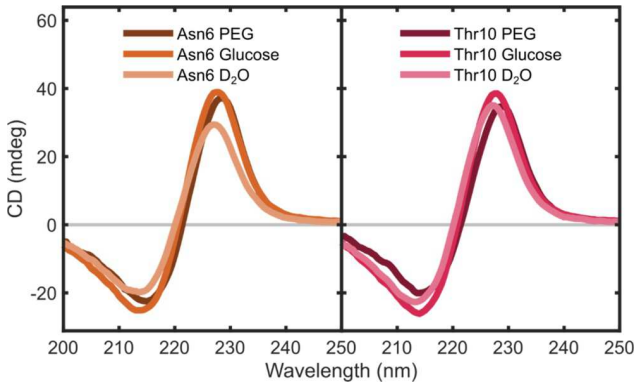

Figure 4. Circular dichroism spectra of each of the mutants under crowded and uncrowded conditions. The *y*-axis is in mdeg and the *x*-axis is wavelength. The spectra remain stable and consistent with published studies, indicative of tryptophan contacts.[30,31,46,47] Normalized spectra, which more easily show trends in position, are available in Section SI II.

hydrogen bonding structure that results in reduced coupling in the antiparallel β-sheet. Notably, the lineshapes are less temperature-sensitive in the PEG solutions as compared to the uncrowded case. This points toward thermal stability of the peptide structure, perhaps due to a confining effect. This is further supported by the baseline widths, which go from narrowest in PEG solution to broadest in glucose solution. The conformational space for the peptide is expanded when crowded with glucose but reduced when crowded with PEG. PEG is generally considered to primarily exert steric or "hard" crowding effects, which is consistent with the observed spectral changes. However, glucose can participate in a wealth of hydrogen bonding interactions which are more described by "soft" crowding. These soft effects can, depending on the attractive or repulsive nature, either exacerbate "hard" effects or counteract/reverse them.[4,45] In the case of TrpZip2 and glucose, the soft interactions destabilize the secondary structure. In other words, the presence of glucose changes the energy landscape of the peptide and solvent such that the native folded structure is less favorable.

Also noteworthy is the fact that the lineshapes of the asparagine-6 mutant show greater susceptibility to heating than the threonine-10 mutant lineshapes, perhaps indicating the asparagine-6 site is important for stabilizing amide I contacts in the peptide. Again, 2D IR studies have shown that the native β-sheet structure can be largely preserved and show these spectral changes.[20] This interpretation is further supported by circular dichroism (Figure 4), as discussed next.

The characteristic CD spectra of TrpZip2 is indicative of strong excitonic coupling between the tryptophan residues.[31,46] The CD spectra collected in this work match those prior studies and show a few interesting features. First, there is a modulation in the peak-to-trough distance of the CD lineshapes, which is a measure of the $\pi-\pi^*$ coupling strength. The glucose crowded TrpZip2 has the strongest coupling for both mutants, whereas the coupling for the D_2O and PEG solutions are reduced. There is also a large drop off in coupling strength for the asparagine-6 mutant in D_2O. When the CD spectra are normalized (Section SI II), a trend in the positions of the line shape extrema emerges, which is that there is a redshift in the peak and trough positions when going from water to glucose to PEG solutions. To our knowledge, there has not been an interpretation provided for peak position shifting of the TrpZip2 CD line shape. Importantly, the CD lineshapes are consistent despite the variable lineshapes of FTIR. Prior studies of TrpZip2 CD and IR spectra have also shown a discrepancy between the TrpZip2 amide I lineshapes and in CD due to the fact that FTIR is dependent on a global arrangement while the TrpZip2 CD is dependent primarily on the tryptophan residue arrangement.[44,47] Combining these observations strengthens the argument of a modified hydrogen bonding structure of the TrpZip2 peptide when crowded with glucose. This modified structure would allow the tryptophan residues to enter a slightly altered state with greater coupling. Ultimately, the present work interprets the IR and CD spectra to indicate that all TrpZip2 mutants and solutions remain in a mostly folded state at room temperature. Importantly, the crowding effects of glucose and PEG are opposite, causing destabilizing and stabilizing behavior, respectively.

III.II. Local Probes in the Steady State. In addition to the global amide I focused spectra taken in D_2O, FTIR spectra were also measured in H_2O to examine the localized azide peak (Figure 5). Doing so highlights the contrast between a generalized interpretation of the local peptide environment and

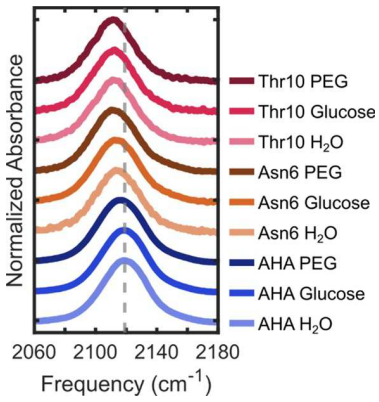

Figure 5. Azide FTIR of the TrpZip2 mutants in crowded and uncrowded solutions. Spectra are normalized by maximum and offset from one another. The dashed gray line indicates the center of the free AHA peak in H_2O as determined by single Gaussian fitting.

https://doi.org/10.1021/acs.jpcb.4c00712
J. Phys. Chem. B 2024, 128, 5310−5319

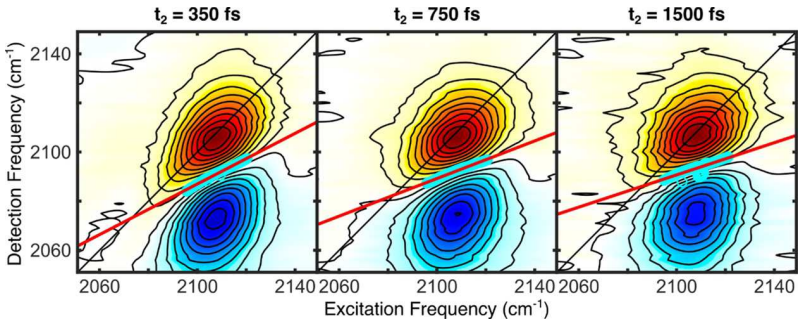

Figure 6. Example 2D IR spectra of the threonine-10 mutant crowded with glucose. The excitation (pump) frequency is on the *x*-axis and the detection (probe) frequency is on the *y*-axis. The $|0\rangle \rightarrow |1\rangle$ transition is shown in red, and the $|1\rangle \rightarrow |2\rangle$ transition is shown in blue. Three different waiting times, t_2, are shown. 2D IR data is interpolated. Nodal points are shown as cyan circles with the red line representing the fit of the nodal line.

a specific one. By monitoring the azide line shape, contrast between different peptide sites and the aqueous bulk is revealed. For these spectra, free AHA is also included as a measure of the bulk environment.

Exploring the azide center frequencies across samples (Figure 4 and Table 1) reveals two specific trends: First, the peaks experience a small redshift upon crowding, with the effect of PEG being greater than glucose. Second, the azide experiences a redshift from the free AHA into to the asparagine-6 site, and then further shifts going to the threonine-10 site. The line width of AHA labels on a peptide has been correlated to the level of solvent exposure of the probe, approximately doubling upon solvent exposure in one instance.[15] In the present work, the greatest observed change is less than 2.5 cm^{-1}. Furthermore, the line widths in the present work correspond approximately to the fully solvent-exposed line widths of prior work (the cited work does not report fwhm).[15] These data might suggest that all the TrpZip2 mutants have solvent-exposed probes. However, another study on the very similar β-azidoalanine probe did not show a significant change in line width upon being buried in an aggregate, even with a large change in center frequency.[48] Perhaps this should be taken as evidence that a broad ensemble does not necessarily preclude the possibility of a buried probe and vice versa. Nevertheless, based on the size and folded structure of the TrpZip2 peptide, the AHA line widths in this work probably correspond to reasonably solvent exposed populations.

There have also been studies on the changes in peak width and more prominently, asymmetry, reported for azide probes due to the existence of a Fermi resonance peak blue-shifted by around 30−40 cm^{-1} from the main peak.[49−51] In some instances, the prominence and width changes due to the resonance have been directly connected to the angular range of motion explored by the bond between the azide and the linking carbon atom.[49,50] Analysis of the molecular dynamics simulations in this work has shown that all measured species have a matching C−N−N angular distribution with a fwhm of 10.5° centered around about 116°, which is not sufficient to explain the subtle differences in FTIR line width (Figure S16).

Returning to the frequency shift, in general, a shift of azide absorption toward lower energies can be correlated with the overall loss of hydrogen bonding or water exposure.[48,52] *Ab initio* calculations have been used to determine the origin of certain spectral features of azides in hydrogen-bonding environments.[16,53] From those studies, three frequency-shift mechanisms are presented. First, the hydrogen-bond angle to the terminal nitrogen; a bond more linear with the azide causes a blueshift (σ-type) and more perpendicular causes a redshift (π-type). Second, hydrogen bonding to the innermost nitrogen causes a blueshift. Third, attractive Coulombic interactions with the middle nitrogen can also induce a blueshift. To add complexity, these contributions can cancel each other out, especially at the protein−water interface, with opposing shifts sometimes happening in tandem.[16] Without treating the system with quantum mechanical calculations, frequency shifting in aqueous environments can be treated with a holistic understanding of the above effects. In this regard, solvent exposure is sufficient to explain the observed trends with the TrpZip2 mutants (Figure 5). When AHA is bound to a peptide, solvent access to the innermost nitrogen is sterically hindered, causing the redshift shown in the peptide samples. This steric interpretation would also imply increased Coulombic interactions with the central nitrogen atom and less σ-type hydrogen bonds with the terminal nitrogen, the effects of which cancel each other. The threonine-10 site is located more centrally in the folded peptide, which explains the magnified redshifting effect with respect to asparagine-6. During crowding, steric effects may reduce the overall presence of water and push the labile probes deeper into the peptide, further enhancing the site-dependent effects, with PEG having a larger effect than glucose. Beyond simply hard steric effects, the glucose hydrogen bonds to the azide are also consistent with a red shift. Glucose can form water-like, but distinct hydrogen bonding environments.[12,54] In the confined space near the peptide, glucose does not have the same ability to penetrate to the innermost nitrogen that water does. Furthermore, depending on azide positioning, glucose may be sterically hindered from forming σ-type hydrogen bonds with the terminal azide.

In combination, these steady-state spectroscopic techniques provide a wealth of insight into the nature of TrpZip2 under crowding conditions. The amide I FTIR and CD spectra provide an overall image of the peptide as an antiparallel β-sheet, stabilized by PEG and destabilized by glucose. The azide FTIR are not sensitive to the peptide conformation, instead reporting more directly on local crowding interactions. This stark contrast highlights the specific advantages of using the azide probe, which provides spectroscopic insight into the solvent and local site, unaffected in this case by the global peptide state. These results also highlight the dimensionality of crowding interactions, with PEG and glucose showing

https://doi.org/10.1021/acs.jpcb.4c00712
J. Phys. Chem. B 2024, 128, 5310−5319

opposing effects at the secondary structure level, but similar structural effects at the site-specific level.

III.III. Subpicosecond Dynamics Around the Local Probe. While the steady-state amide and azide steady-state spectra provide a structural perspective on the protein and local solvent environment, an important quality of water within crowded biological systems is the hydrogen bond network. Because many of the local hydrogen bond behaviors occur on the subpicosecond to picosecond time scale, this regime can be measured to give a more complete picture of the crowded environment around TrpZip2. Therefore, time-resolved 2D IR spectra of the azide were collected, with Figure 6 showing a representative set of spectra for the threonine-10 mutants crowded with glucose.

The initial diagonal elongation of the $|0\rangle \rightarrow |1\rangle$ peak (red peak) shows a correlation between the excitation frequency and detection frequency. The relaxation of the nodal line is linked to the frequency fluctuation correlation function. As the time between excitation and detection increases, the local environment changes and the correlation is lost, referred to as spectral diffusion.[55] The positive and negative peaks of azidohomoalanine are significantly less diagonally elongated after 1500 fs. The slope of the nodal points between the positive and negative peak can be used to track spectral diffusion through nodal line slope (NLS) analysis.[35] The time evolution of the spectra can be interpreted via an exponential frequency fluctuation correlation function (FFCF), $C(t)$, presented as an exponential decay with explicit inertial and static components (eq 1). The inertial components manifest as an initial offset between 1 and the first NLS value, the static inhomogeneous component is an offset between 0 and the final NLS values, and the dynamic stochastic portion is captured in the exponential decay. T_2 is the homogeneous dephasing time, Δ_ω represents the amplitude of frequency fluctuations, t_2 is the waiting time, τ is the correlation time, and Δ_0 is the static inhomogeneity.

$$C(t) = \langle \delta\omega(t_2)\delta\omega(0)\rangle = \frac{\delta(t_2)}{T_2} + \Delta_\omega^2 e^{-t_2/\tau} + \Delta_0^2 \quad (1)$$

The nodal line slope is fit to an exponential decay, where the static inhomogeneity become a unitless scalar, a_0, because the slope of the line is unitless. Fortunately, any Δ_i, such as the static inhomogeneity, can be represented in wavenumbers by using the Gaussian width of the FTIR peak, σ, and the unitless amplitude of the NLS component, a_i, (eq 2).[56] By doing so, the total line width is accounted for in comparison between different chemical environments.

$$\Delta_i = \sigma \times \sqrt{a_i} \quad (2)$$

The extracted correlations times and static inhomogeneities from the nodal line slopes are shown in Figure 7.

The correlation time tracks the frequency fluctuations resulting from the subpicosecond solvent dynamics of and around the probe molecule. The free AHA lineshapes show little to no change in dynamics upon the addition of glucose and PEG. This trend is replicated with the threonine-10 lineshapes, with dynamics of 400 fs. In contrast, the asparagine-6 undergoes a slowdown upon crowding. The static inhomogeneity again shows a contrast between asparagine-6 and the rest of the spectra. The free AHA spectra show increasing static inhomogeneity from 7.8 to 9.1 cm^{-1} upon crowding, while the threonine-10 line shape shows a similar

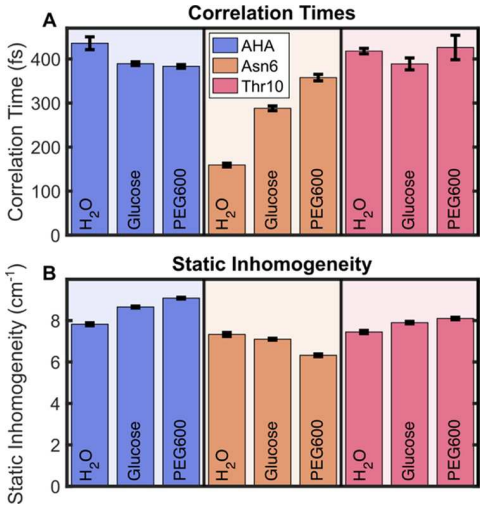

Figure 7. (A) Frequency fluctuation correlation decay times of azidohomoalanine (AHA), TrpZip2-Asn6AHA, and TrpZip2-Thr10AHA in water as well as glucose and PEG crowders. The decays are extracted via NLS fitting of the 2D spectra. (B) Magnitudes of the static inhomogeneous component extracted from NLS fitting and FTIR widths. All error bars are determined by bootstrapping.

trend, increasing from 7.4 to 8.1 cm^{-1}. The asparagine-6 spectra decrease in static inhomogeneity upon crowding, going from 7.3 to 6.3 cm^{-1}. In all cases, PEG has a greater perturbation on the ultrafast dynamics than glucose, which is in agreement with previous work.[12]

It should be noted that prior studies on azidohomoalanine have been variable in the range of time scales and inhomogeneity. A prior 2D IR study of the AHA label on peptides showed a correlation time which is considerably slower, about 3 ps.[14] However, theoretical work has shown AHA FFCFs with correlation times on the order of a few hundred femtoseconds or less,[16] and other studies on azido probes in aqueous environments have found correlation times between 0.5 and 2 ps.[26,27,51,57,58] Still, this prior study found that consistent correlation times for the AHA peptide label under different conditions were due to consistent solvent exposure.[14] This implies that the variable correlation time of the asparagine-6 site label could be due to changing hydration under crowded conditions. In general, experimental and theoretical work for AHA combined with knowledge about water dynamics show that correlation times on this time scale are driven by azide motions, hindered water motions, and hydrogen bond motions.[14,16,59] Even though there are consistent correlation times between the free AHA and threonine-10 site, the convolved nature of the dynamics makes it difficult to uncover the origin of the frequency fluctuations in both probes. Whether or not the origin of the fluctuations is the same, both instances show little perturbation from crowding. This could be due to interactions with hydrophilic residues. There has been precedent which indicates that, at least for glucose, dynamics at hydrophilic interfaces can remain unaltered under high crowder concentrations.[54] And hydrophilic sites on proteins have been shown to preserve water networks under crowding conditions.[60] While the threonine-10 site is in the core of the peptide, the side chain extends into a region with hydrophilic residues.

One surprising behavior of the asparagine-6 site is that the measured dynamics under uncrowded conditions are faster

https://doi.org/10.1021/acs.jpcb.4c00712
J. Phys. Chem. B 2024, 128, 5310−5319

than those of free AHA. Again, these fluctuations are due to a combination of many factors and the asparagine-6 site and free AHA dynamics could be primarily driven by different processes, e.g., one by azide motions and the other by water. These motions have been deconvolved in the past through quantum mechanics/molecular mechanics (QM/MM) simulations, which use *ab initio* calculations to determine energetic contributions from different sources accurately. This deconvolution is not possible with an ensemble measurement such as 2D IR.[16] Regardless, the slowdown in dynamics around the asparagine-6 site is consistent with a disordering of crowder-proximal water, which has been shown to occur in previous studies with glucose and PEG.[12]

As for the inhomogeneity, QM/MM has been used to assign slower (quasi-static) dynamics to interactions between the middle azide nitrogen and peptide/protein contacts, though these contacts were facilitated by a lack of solvation due to protein geometry and hydrophobicity.[16] Some 2D IR measurements, in contrast, have concluded that there are situations where bound AHA residues can interact with interfacial water in a similar manner to bulk water while simultaneously maintaining middle nitrogen contacts.[14] To interpret the results of the free AHA and threonine-10 sites, recall the preliminary interpretation of the FTIR results, which suggested that crowders may reduce the innermost nitrogen hydrogen bonding, drive the azide into the peptide, and reduce the conformational space of water around the terminal azide nitrogen. A similar result was found in a previous 2D IR crowding study, which showed that water dynamics are progressively arrested under increased crowder concentrations, and, in their case, slower peptide dynamics were correlated.[61] These changes were attributed to a reduction in hydration and number of possible water configurations upon crowding. This model can be completely applied to the free AHA and threonine-10 samples. In these cases, the static inhomogeneity increases as the crowding effect increases, which is consistent with having a more buried probe. Additionally, increased middle nitrogen contacts are associated with reduced hydration.[16] In the case of the asparagine-6 site, molecular dynamics simulations have shown that the turn region of other TrpZips is comparatively dehydrated with respect to the strands (and bulk) attributed to increased flexibility.[62] In a cursory examination, increased flexibility is aligned with the less spectrally stable (less statically inhomogeneous) azide at the asparagine-6 site. However, it is difficult to reconcile the progressive decrease in inhomogeneity from water to glucose to PEG with the observed changes in secondary structure between glucose and PEG (Figure 7). Granted, the effect of crowding on the turn is not measured by either CD or the β-sheet character of the amide I region.

One additional parameter that can be extracted from ultrafast spectroscopy is the vibrational lifetime of azide for each experimental conditional. Changes in vibrational lifetime can be due to changes in the coupling to bath states. As such, a more buried vibrational probe might be expected to have a longer vibrational lifetime. In the Supporting Information, the vibrational lifetime of AHA was determined to be on the order of 0.8 ± 0.2 to 1.2 ± 0.2 ps, with the threonine-10 site having the longest lifetime. This is consistent with the proposed solvent exposure hypothesis.

To aid in the interpretation of the 2D IR spectra, classical MD simulations were performed as described in the Section II. These simulations have the advantage of atomistic detail. Considering the interpretation of FTIR and 2D IR lineshapes involves desolvation of the azide probe when undergoing crowding conditions, the distance between the azide nitrogens and each of their five closest oxygen atoms was computed as a measure of local solvation environment around the probe. The oxygen atoms are the primary species that interact with the middle nitrogen, and they also form a proxy for measuring hydrogen-bonding with the innermost and terminal nitrogens. In other words, the oxygen atom distances represent global measure of the overall h-bonding and other Coulombic interactions. The resulting histograms (Figure 8) provide insight on these effects.

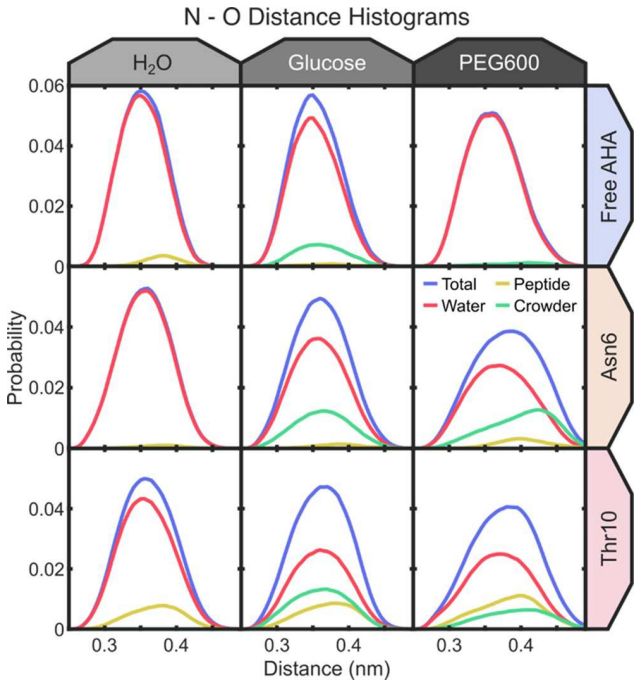

Figure 8. Histograms of the distance between azide nitrogen atoms and the nearest five oxygen atoms. The *x*-axis is distance in nanometers and the *y*-axis is a probability normalized so the integral is 1. The oxygen atoms are presented as the oxygen atoms on the peptide (or free AHA), those present on the crowder, the oxygen in water, and the total. These histograms are computed from the 20 100 ps trajectories for the peptides and from the 1 ns trajectory for the free AHA (see Section II).

The total number of oxygen atoms is indicated by the blue line. Because each vertical axis is a probability and each distribution contains five oxygen atoms, the height of the total line corresponds inversely to the width of the distribution. Each total line also starts at approximately the same lower bound of distance. With this in mind, it is clear to see that the addition of crowder results in a wider distribution of oxygen distances, with a greater population being further from the azide; this is interpreted as desolvation. Furthermore, PEG, like in the other experiments, has a greater effect than glucose. In addition, the distributions of oxygens around the threonine-10 site are either wider or right-shifted compared to the asparagine-6 site, which itself has distributions wider and further shifted than the free AHA. This reduction in oxygen interaction matches directly with the red-shifted peaks measured from FTIR. Another notable trend in the histograms is that the threonine-10 site shows significantly more

https://doi.org/10.1021/acs.jpcb.4c00712
J. Phys. Chem. B 2024, 128, 5310−5319

interactions with the peptide oxygens, confirming the status of the threonine-10 site as more buried. In both the asparagine-6 site and threonine-10 site, interactions with the peptide increase from water to glucose solution to PEG solution, again consistent with the probe becoming more buried. There is also a difference between the crowder oxygen distances of glucose and PEG. The glucose distances are more centered around 0.35 nm, which is a common cutoff for hydrogen bonding in aqueous environments,[63] while the PEG distances are skewed to the right, indicating non-H-bonding interactions.

In summary, the dynamic and static spectral components indicate that each probe site samples a unique environment of water and azido-peptide contacts, which are modulated by the presence of crowders. Some of the trends in frequency shifts and dynamics are well explained by current theories of azido solvation, while other trends are less intuitive. There are clear indications that, on the site-specific level, both PEG and glucose crowders are driving desolvation of the azide probe. This has important implications in the use of azidohomoalanine as a spectroscopic probe on proteins. Rather than being able to rely on AHA as solely a reporter of the nonpeptide local environment, it will be important to note how some changes in spectral response may be entirely explained by changes in the probe position. In other words, a change in the azide spectra may not actually be due to a change in the region of interest.

IV. SUMMARY AND CONCLUSIONS

In summary, the results of these studies show azidohomoalanine as a unique reporter of the peptide and its environment on a site-specific basis. Dynamics measured through 2D IR spectroscopy were able to provide experimental evidence for both perturbed and unperturbed local environments around TrpZip2 upon crowding. The dynamics are stable for the free probe and the probe positioned in the core of the peptide, while the probe undergoes a dynamic slowdown during crowding in the more complex turn region. However, while AHA can be a sensitive local reporter, global changes in the peptide may not be evident in azide spectra. For example, large changes in interstrand coupling were observed in the amide I region under glucose crowding, but these did not have a large effect on the azido stretch. These findings underscore previous work with azide probes, which have demonstrated that the positioning of the probe is critically important to achieving a sensitive spectral response to the environment.[64] On top of these considerations, this work has demonstrated that some azide spectral features remain complex to explain in the intricate context of peptide local environment. Even though molecular dynamics simulations can provide some insight on the sources of the spectral features, more advanced computational techniques that can more accurately measure fluctuations in the energy of the azide group or directly output frequency shifts would be useful in determining the exact nature of the azide behavior. Nonetheless, these results also highlight an important scale-dependent crowding behavior. Often, thermodynamic effects on proteins are viewed as either stabilizing or destabilizing. However, the results of this study reveal that perturbations to the energy landscape may be more accurately described by a multiscale model. In other words, the thermodynamic balance that drives changes on a secondary structure level is different than that which drives changes on a site-specific level. Previous work on crowding has certainly shown that, among hard effects, a crowder can transition between hard-sphere and confinement behavior as its molecular weight increases.[65] Naturally, these energetic contributions are somewhat relativistic and a confining crowder to a smaller molecule may be a hard-sphere to a macromolecule. In the same way, a single residue or small region on a protein will experience crowding in a different way than the whole molecule. Reincorporating the idea that soft interactions can aggravate, pacify, or reverse hard interactions, it becomes apparent that this interplay takes course uniquely on every length scale. In the present work, there were large differences between the hydrogen-bonding, water-like glucose, and the relatively "hard" PEG. While both crowders induced steric pressure and dehydration on the amino acid level, they had opposing effects on the β-sheet. However, these systems are grossly simplified compared to a biological context. In the cellular environment, there are crowders and osmolytes of every relative size, each of them exerting unique forces at every level of scale of the molecule of interest.

■ ASSOCIATED CONTENT

Supporting Information

The Supporting Information is available free of charge at https://pubs.acs.org/doi/10.1021/acs.jpcb.4c00712.

Additional FTIR and CD plots. All 2D IR spectra. Fitting results and vibrational lifetimes from 2D IR. Angle distributions from molecular dynamics simulations (PDF)

■ AUTHOR INFORMATION

Corresponding Author

Carlos R. Baiz − *Department of Chemistry, University of Texas, Austin, Texas 78712, United States;* orcid.org/0000-0003-0699-8468; Email: cbaiz@cm.utexas.edu

Author

Joseph C. Shirley − *Department of Chemistry, University of Texas, Austin, Texas 78712, United States*

Complete contact information is available at: https://pubs.acs.org/10.1021/acs.jpcb.4c00712

Notes

The authors declare no competing financial interest.

■ ACKNOWLEDGMENTS

This work is supported by the National Science Foundation (CHE-1847199) and the Welch Foundation (F-1891).

■ REFERENCES

(1) Ellis, R. J.; Minton, A. P. Join the Crowd. *Nature* **2003**, *425* (6953), 27−28.

(2) Feig, M.; Yu, I.; Wang, P.; Nawrocki, G.; Sugita, Y. Crowding in Cellular Environments at an Atomistic Level from Computer Simulations. *J. Phys. Chem. B* **2017**, *121* (34), 8009−8025.

(3) Zhou, H.-X.; Rivas, G.; Minton, A. P. Macromolecular Crowding and Confinement: Biochemical, Biophysical, and Potential Physiological Consequences. *Annu. Rev. Biophys.* **2008**, *37*, 375−397.

(4) Sarkar, M.; Li, C.; Pielak, G. J. Soft Interactions and Crowding. *Biophys Rev.* **2013**, *5* (2), 187−194.

(5) Santero, S. P.; Favretto, F.; Zanzoni, S.; Chignola, R.; Assfalg, M.; D'Onofrio, M. Effects of Macromolecular Crowding on a Small Lipid Binding Protein Probed at the Single-Amino Acid Level. *Arch. Biochem. Biophys.* **2016**, *606*, 99−110.

(6) Grebenkov, D. S.; Goddard, Y. A.; Diakova, G.; Korb, J.-P.; Bryant, R. G. Dimensionality of Diffusive Exploration at the Protein Interface in Solution. *J. Phys. Chem. B* **2009**, *113* (40), 13347−13356.
(7) Halle, B. Protein Hydration Dynamics in Solution: A Critical Survey. *Philos. Trans. R. Soc., B* **2004**, *359* (1448), 1207−1224, DOI: 10.1098/rstb.2004.1499.
(8) Shin, S.; Willard, A. P. Water's Interfacial Hydrogen Bonding Structure Reveals the Effective Strength of Surface−Water Interactions. *J. Phys. Chem. B* **2018**, *122*, 6781−6789, DOI: 10.1021/acs.jpcb.8b02438.
(9) Bellissent-Funel, M.-C.; Hassanali, A.; Havenith, M.; Henchman, R.; Pohl, P.; Sterpone, F.; van der Spoel, D.; Xu, Y.; Garcia, A. E. Water Determines the Structure and Dynamics of Proteins. *Chem. Rev.* **2016**, *116* (13), 7673−7697.
(10) Ball, P. Water Is an Active Matrix of Life for Cell and Molecular Biology. *Proc. Natl. Acad. Sci. U.S.A.* **2017**, *114* (51), 13327−13335.
(11) Ball, P. Water as an Active Constituent in Cell Biology. *Chem. Rev.* **2008**, *108* (1), 74−108.
(12) You, X.; Shirley, J. C.; Lee, E.; Baiz, C. R. Short- and Long-Range Crowding Effects on Water's Hydrogen Bond Networks. *Cell Rep. Phys. Sci.* **2021**, *2* (5), No. 100419.
(13) Baiz, C. R.; Reppert, M.; Tokmakoff, A. An Introduction to Protein 2D IR Spectroscopy. In *Ultrafast Infrared Vibrational Spectroscopy*; Fayer, M. D., Ed.; Taylor & Francis: New York, 2013; pp 361−403.
(14) Bloem, R.; Koziol, K.; Waldauer, S. A.; Buchli, B.; Walser, R.; Samatanga, B.; Jelesarov, I.; Hamm, P. Ligand Binding Studied by 2D IR Spectroscopy Using the Azidohomoalanine Label. *J. Phys. Chem. B* **2012**, *116* (46), 13705−13712.
(15) Taskent-Sezgin, H.; Chung, J.; Banerjee, P. S.; Nagarajan, S.; Dyer, R. B.; Carrico, I.; Raleigh, D. P. Azidohomoalanine: A Conformationally Sensitive IR Probe of Protein Folding Protein Structure and Electrostatics. *Angew. Chem., Int. Ed.* **2010**, *49* (41), 7473−7475.
(16) Choi, J. H.; Raleigh, D.; Cho, M. Azido Homoalanine Is a Useful Infrared Probe for Monitoring Local Electrostatistics and Sidechain Solvation in Proteins. *J. Phys. Chem. Lett.* **2011**, *2* (17), 2158−2162, DOI: 10.1021/jz200980g.
(17) Zanobini, C.; Bozovic, O.; Jankovic, B.; Koziol, K. L.; Johnson, P. J. M.; Hamm, P.; Gulzar, A.; Wolf, S.; Stock, G. Azidohomoalanine: A Minimally Invasive, Versatile, and Sensitive Infrared Label in Proteins To Study Ligand Binding. *J. Phys. Chem. B* **2018**, *122* (44), 10118−10125.
(18) Smith, A. W.; Tokmakoff, A. Amide I Two-Dimensional Infrared Spectroscopy of β-Hairpin Peptides. *J. Chem. Phys.* **2007**, *126* (4), No. 045109.
(19) Jones, K. C.; Peng, C. S.; Tokmakoff, A. Folding of a Heterogeneous β-Hairpin Peptide from Temperature-Jump 2D IR Spectroscopy. *Proc. Natl. Acad. Sci. U.S.A.* **2013**, *110* (8), 2828−2833.
(20) Smith, A. W.; Chung, H. S.; Ganim, Z.; Tokmakoff, A. Residual Native Structure in a Thermally Denatured β-Hairpin. *J. Phys. Chem. B* **2005**, *109* (36), 17025−17027.
(21) Barth, A.; Haris, P. *Biological and Biomedical Infrared Spectroscopy*; IOS Press: Amsterdam, 2009.
(22) Lasch, P.; Kneipp, J. *Biomedical Vibrational Spectroscopy*, 1st ed.; John Wiley & Sons, Incorporated: Hoboken, 2008.
(23) Baiz, C. R.; Błasiak, B.; Bredenbeck, J.; Cho, M.; Choi, J. H.; Corcelli, S. A.; Dijkstra, A. G.; Feng, C. J.; Garrett-Roe, S.; Ge, N. H.; et al. Vibrational Spectroscopic Map, Vibrational Spectroscopy, and Intermolecular Interaction. *Chem. Rev.* **2020**, *120* (15), 7152−7218.
(24) de Moliner, F.; Knox, K.; Gordon, D.; Lee, M.; Tipping, W. J.; Geddis, A.; Reinders, A.; Ward, J. M.; Oparka, K.; Vendrell, M. A Palette of Minimally Tagged Sucrose Analogues for Real-Time Raman Imaging of Intracellular Plant Metabolism. *Angew. Chem.* **2021**, *133* (14), 7715−7720.
(25) Debets, M. F.; van Hest, J. C. M.; Rutjes, F. P. J. T. Bioorthogonal Labelling of Biomolecules: New Functional Handles and Ligation Methods. *Org. Biomol. Chem.* **2013**, *11* (38), 6439−6455.
(26) Tucker, M. J.; Gai, X. S.; Fenlon, E. E.; Brewer, S. H.; Hochstrasser, R. M. 2D IR Photon Echo of Azido-Probes for Biomolecular Dynamics. *Phys. Chem. Chem. Phys.* **2011**, *13* (6), 2237−2241.
(27) Thielges, M. C.; Axup, J. Y.; Wong, D.; Lee, H. S.; Chung, J. K.; Schultz, P. G.; Fayer, M. D. Two-Dimensional IR Spectroscopy of Protein Dynamics Using Two Vibrational Labels: A Site-Specific Genetically Encoded Unnatural Amino Acid and an Active Site Ligand. *J. Phys. Chem. B* **2011**, *115* (38), 11294−11304.
(28) Markiewicz, B. N.; Oyola, R.; Du, D.; Gai, F. Aggregation Gatekeeper and Controlled Assembly of Trpzip β-Hairpins. *Biochemistry* **2014**, *53* (7), 1146−1154.
(29) Krejtschi, C.; Huang, R.; Keiderling, T. A.; Hauser, K. Time-Resolved Temperature-Jump Infrared Spectroscopy of Peptides with Well-Defined Secondary Structure: A Trpzip β-Hairpin Variant as an Example. *Vib. Spectrosc.* **2008**, *48* (1), 1−7.
(30) Yang, W. Y.; Pitera, J. W.; Swope, W. C.; Gruebele, M. Heterogeneous Folding of the Trpzip Hairpin: Full Atom Simulation and Experiment. *J. Mol. Biol.* **2004**, *336* (1), 241−251.
(31) Cochran, A. G.; Skelton, N. J.; Starovasnik, M. A. Tryptophan Zippers: Stable, Monomeric β-Hairpins. *Proc. Natl. Acad. Sci. U.S.A.* **2001**, *98* (10), 5578−5583.
(32) Maia, R. N. A.; Mitra, S.; Baiz, C. R. Extracting Accurate Infrared Lineshapes from Weak Vibrational Probes at Low Concentrations. *MethodsX* **2023**, *11*, No. 102309.
(33) Edington, S. C.; Gonzalez, A.; Middendorf, T. R.; Halling, D. B.; Aldrich, R. W.; Baiz, C. R. Coordination to Lanthanide Ions Distorts Binding Site Conformation in Calmodulin. *Proc. Natl. Acad. Sci. U.S.A.* **2018**, *115* (14), E3126−E3134.
(34) Robben, K. C.; Cheatum, C. M. Edge-Pixel Referencing Suppresses Correlated Baseline Noise in Heterodyned Spectroscopies. *J. Chem. Phys.* **2020**, *152* (9), No. 094201.
(35) Kwac, K.; Cho, M. Molecular Dynamics Simulation Study of N-Methylacetamide in Water. II. Two-Dimensional Infrared Pump−Probe Spectra. *J. Chem. Phys.* **2003**, *119* (4), 2256−2263.
(36) Bekker, H.; Berendsen, H.; Dijkstra, E.; Achterop, S.; Van Drunen, R.; Van der Spoel, D.; Sijbers, A.; Keegstra, H.; Reitsma, B.; Renardus, M. In *Gromacs: A Parallel Computer for Molecular Dynamics Simulations*, 4th International Conference on Computational Physics; World Scientific Publishing, 1993; pp 252−256.
(37) Abraham, M. J.; Murtola, T.; Schulz, R.; Páll, S.; Smith, J. C.; Hess, B.; Lindahl, E. GROMACS: High Performance Molecular Simulations through Multi-Level Parallelism from Laptops to Supercomputers. *SoftwareX* **2015**, *1*−*2*, 19−25.
(38) Huang, J.; Rauscher, S.; Nawrocki, G.; Ran, T.; Feig, M.; de Groot, B. L.; Grubmüller, H.; MacKerell, A. D. CHARMM36m: An Improved Force Field for Folded and Intrinsically Disordered Proteins. *Nat. Methods* **2017**, *14* (1), 71−73.
(39) Brooks, B. R.; Brooks, C. L., III; Mackerell, A. D., Jr.; Nilsson, L.; Petrella, R. J.; Roux, B.; Won, Y.; Archontis, G.; Bartels, C.; Boresch, S.; et al. CHARMM: The Biomolecular Simulation Program. *J. Comput. Chem.* **2009**, *30* (10), 1545−1614.
(40) Jo, S.; Kim, T.; Iyer, V. G.; Im, W. CHARMM-GUI: A Web-Based Graphical User Interface for CHARMM. *J. Comput. Chem.* **2008**, *29* (11), 1859−1865.
(41) Lee, J.; Cheng, X.; Swails, J. M.; Yeom, M. S.; Eastman, P. K.; Lemkul, J. A.; Wei, S.; Buckner, J.; Jeong, J. C.; Qi, Y.; et al. CHARMM-GUI Input Generator for NAMD, GROMACS, AMBER, OpenMM, and CHARMM/OpenMM Simulations Using the CHARMM36 Additive Force Field. *J. Chem. Theory Comput.* **2016**, *12* (1), 405−413.
(42) Kim, S.; Lee, J.; Jo, S.; Brooks, C. L., III; Lee, H. S.; Im, W. CHARMM-GUI Ligand Reader and Modeler for CHARMM Force Field Generation of Small Molecules. *J. Comput. Chem.* **2017**, *38* (21), 1879−1886.
(43) Martínez, L.; Andrade, R.; Birgin, E. G.; Martínez, J. M. PACKMOL: A package for building initial configurations for molecular dynamics simulations. *J. Comput. Chem.* **2009**, *30* (13), 2157−2164.

https://doi.org/10.1021/acs.jpcb.4c00712
J. Phys. Chem. B 2024, 128, 5310−5319

(44) Wang, T.; Xu, Y.; Du, D.; Gai, F. Determining β-Sheet Stability by Fourier Transform Infrared Difference Spectra. *Biopolymers* **2004**, *75* (2), 163−172.
(45) You, X.; Baiz, C. R. Importance of Hydrogen Bonding in Crowded Environments: A Physical Chemistry Perspective. *J. Phys. Chem. A* **2022**, *126* (35), 5881−5889.
(46) Grishina, I. B.; Woody, R. W. Contributions of Tryptophan Side Chains to the Circular Dichroism of Globular Proteins: Exciton Couplets and Coupled Oscillators. *Faraday Discuss.* **1994**, *99* (0), 245−262.
(47) Wu, L.; McElheny, D.; Huang, R.; Keiderling, T. A. Role of Tryptophan-Tryptophan Interactions in Trpzip β-Hairpin Formation, Structure, and Stability. *Biochemistry* **2009**, *48* (43), 10362−10371.
(48) Oh, K.-I.; Lee, J.-H.; Joo, C.; Han, H.; Cho, M. β-Azidoalanine as an IR Probe: Application to Amyloid Aβ(16−22) Aggregation. *J. Phys. Chem. B* **2008**, *112* (33), 10352−10357.
(49) Varner, C.; Zhou, X.; Saxman, Z. K.; Leger, J. D.; Jayawickramarajah, J.; Rubtsov, I. V. Azido Alkanes as Convenient Reporters for Mobility within Lipid Membranes. *Chem. Phys.* **2018**, *512*, 20−26.
(50) Islam, M. M.; Nawagamuwage, S. U.; Parshin, I. V.; Richard, M. C.; Burin, A. L.; Rubtsov, I. V. Probing the Hydrophobic Region of a Lipid Bilayer at Specific Depths Using Vibrational Spectroscopy. *J. Am. Chem. Soc.* **2023**, *145* (48), 26363−26373.
(51) Park, J. Y.; Kwon, H.-J.; Mondal, S.; Han, H.; Kwak, K.; Cho, M. Two-Dimensional IR Spectroscopy Reveals a Hidden Fermi Resonance Band in the Azido Stretch Spectrum of β-Azidoalanine. *Phys. Chem. Chem. Phys.* **2020**, *22* (34), 19223−19229.
(52) Gai, X. S.; Coutifaris, B. A.; Brewer, S. H.; Fenlon, E. E. A Direct Comparison of Azide and Nitrile Vibrational Probes. *Phys. Chem. Chem. Phys.* **2011**, *13* (13), 5926−5930.
(53) Choi, J. H.; Oh, K. I.; Cho, M. Azido-Derivatized Compounds as IR Probes of Local Electrostatic Environment: Theoretical Studies. *J. Chem. Phys.* **2008**, *129* (17), No. 124503.
(54) You, X.; Lee, E.; Xu, C.; Baiz, C. R. Molecular Mechanism of Cell Membrane Protection by Sugars: A Study of Interfacial H-Bond Networks. *J. Phys. Chem. Lett.* **2021**, *12*, 9602−9607, DOI: 10.1021/acs.jpclett.1c02451.
(55) Hamm, P.; Zanni, M. *Concepts and Methods of 2D Infrared Spectroscopy*; Cambridge University Press: New York, 2011.
(56) Kwak, K.; Park, S.; Finkelstein, I. J.; Fayer, M. D. Frequency-Frequency Correlation Functions and Apodization in Two-Dimensional Infrared Vibrational Echo Spectroscopy: A New Approach. *J. Chem. Phys.* **2007**, *127* (12), No. 124503.
(57) He, X.; Xu, F.; Yu, P.; Wu, Y.; Wang, F.; Zhao, Y.; Wang, J. Solvent-Dependent Structural Dynamics of an Azido-Platinum Complex Revealed by Linear and Nonlinear Infrared Spectroscopy. *Phys. Chem. Chem. Phys.* **2018**, *20* (15), 9984−9996.
(58) Dutta, S.; Li, Y.-L.; Rock, W.; Houtman, J. C. D.; Kohen, A.; Cheatum, C. M. 3-Picolyl Azide Adenine Dinucleotide as a Probe of Femtosecond to Picosecond Enzyme Dynamics. *J. Phys. Chem. B* **2012**, *116* (1), 542−548.
(59) Laage, D.; Elsaesser, T.; Hynes, J. T. Water Dynamics in the Hydration Shells of Biomolecules. *Chem. Rev.* **2017**, *117* (16), 10694−10725.
(60) Harada, R.; Sugita, Y.; Feig, M. Protein Crowding Affects Hydration Structure and Dynamics. *J. Am. Chem. Soc.* **2012**, *134* (10), 4842−4849.
(61) King, J. T.; Arthur, E. J.; Brooks, C. L. I.; Kubarych, K. J. Crowding Induced Collective Hydration of Biological Macromolecules over Extended Distances. *J. Am. Chem. Soc.* **2014**, *136* (1), 188−194.
(62) Gupta, M.; Khatua, P.; Chakravarty, C.; Bandyopadhyay, S. Hydration Behavior along the Folding Pathways of Trpzip4, Trpzip5 and Trpzip6. *J. Phys. Chem. B* **2018**, *122* (5), 1560−1572.
(63) Sciortino, F.; Fornili, S. L. Hydrogen Bond Cooperativity in Simulated Water: Time Dependence Analysis of Pair Interactions. *J. Chem. Phys.* **1989**, *90* (5), 2786−2792.
(64) van Wilderen, L. J. G. W.; Kern-Michler, D.; Müller-Werkmeister, H. M.; Bredenbeck, J. Vibrational Dynamics and Solvatochromism of the Label SCN in Various Solvents and Hemoglobin by Time Dependent IR and 2D-IR Spectroscopy. *Phys. Chem. Chem. Phys.* **2014**, *16* (36), 19643−19653.
(65) Miklos, A. C.; Li, C.; Sharaf, N. G.; Pielak, G. J. Volume Exclusion and Soft Interaction Effects on Protein Stability under Crowded Conditions. *Biochemistry* **2010**, *49* (33), 6984−6991.

https://doi.org/10.1021/acs.jpcb.4c00712
J. Phys. Chem. B 2024, 128, 5310−5319